

U.S. DEPARTMENT OF THE INTERIOR

U.S. GEOLOGICAL SURVEY

Origin and Ages of Mineralization of Bayan Obo, the World's Largest  
Rare Earth Ore Deposit, Inner Mongolia, China

by

E.C.T. Chao<sup>1</sup>, Mitsunobu Tatsumoto<sup>2</sup>, R.L. Erickson<sup>2</sup>, J.A. Minkin<sup>1</sup>, J.M. Back<sup>1</sup>,  
R.V. Buden<sup>3</sup>, P.M. Okita<sup>4</sup>, Hou Zonglin<sup>5</sup>, Meng Qingrun<sup>5</sup>, Ren Yingchen<sup>5</sup>, Sun  
Weijun<sup>5</sup>, E.H. McKee<sup>6</sup>, Brent Turrin<sup>6</sup>, Wang Junwen<sup>2</sup>, Li Xibin<sup>2</sup>, and C.A. Edwards<sup>1</sup>

Open-File Report 90-538

This report is preliminary and has not been reviewed for conformity with U.S. Geological Survey editorial standards and stratigraphic nomenclature. Any use of trade, product, or firm names is for descriptive purposes only and does not imply endorsement by the U.S. Government.

<sup>1</sup>USGS Reston, VA

<sup>2</sup>USGS Denver, CO

<sup>3</sup>Present address, Idaho National Engineering Laboratories, Idaho Falls, ID

<sup>4</sup>Present address, BHP-Utah Intl., Inc., Herndon, VA

<sup>5</sup>Tianjin Geological Research Academy, China

<sup>6</sup>USGS Menlo Park, CA

## CONTENTS

	Page
Abstract	1
Introduction	1
Location and geologic setting	1
Mineral paragenetic sequence and ages of mineralization	2
Comparison of Bayan Obo mineral characteristics with those of known magmatic origin	5
Conclusions	5
References and notes	7

## TABLES

Table 1. Chemical compositions and ages of selected Bayan Obo minerals	4
Table 2. General comparison of mineral characteristics between Bayan Obo and carbonatites	6

## ILLUSTRATIONS

Captions for figures	9
Figure 1. Geologic map of the Bayan Obo area	10
Figures 2-5. Photograph and photomicrographs showing textural relationships of Bayan Obo minerals	11

ORIGIN AND AGES OF MINERALIZATION OF BAYAN OBO,  
THE WORLD'S LARGEST RARE EARTH ORE DEPOSIT,  
INNER MONGOLIA, CHINA

EDWARD C.T. CHAO, MITSUNOBU TATSUMOTO, RALPH L. ERICKSON, JEAN A. MINKIN, JUDITH M. BACK, ROSEMARY V. BUDEN, PATRICK M. OKITA, HOU ZONGLIN, MENG QINGRUN, REN YINGCHEN, SUN WEIJUN, EDWIN H. MCKEE, BRENT TURRIN, WANG JUNWEN, LI XIBIN, and CHERYL A. EDWARDS

Abstract. The origin of Bayan Obo, the world's largest known rare-earth-element (REE) ore deposit, has been a subject of geologic interest and speculation. Recent field and laboratory observations support the early conclusion that the Middle Proterozoic host rock of the Bayan Obo ores is not a carbonatite, but a metamorphosed, sedimentary dolomitized limestone. Petrographic textural analysis indicates that the ores are epigenetic, hydrothermal and metasomatic in origin. Radioisotopic data together with the textural analysis show that the principal episodes of mineralization for this unique deposit probably began about 800 Ma and continued to at least 425 Ma, a span of about 400 million years.

Introduction. The use of rare earth elements (REEs) in high technology (for example high-strength ceramics, catalytic functions, permanent magnets, phosphors in video displays, and high-temperature superconductors) (1) makes the occurrence of these elements of increasing economic interest worldwide. Bayan Obo, the world's largest known REE deposit, with inferred reserves of more than 30 million metric tons of rare earth oxides ( $RE_2O_3$ ) (2), has until recently been of extremely limited access for study by the international scientific community.

Five hypotheses for the origin of the Bayan Obo deposit have been proposed (3): a) high-temperature hydrothermal metasomatism related to Hercynian granitic rocks that are widespread in the mine region, b) and c) sabkha sedimentary syngensis preceding regional metamorphism with or without additional hydrothermal metasomatism, d) magmatic carbonatite, and e) exhalative volcanogenic carbonatite sedimentation. Results reported below support a sixth hypothesis, a late Proterozoic to Caledonian age epigenetic, hydrothermal, metasomatic origin.

Location and geologic setting. The Bayan Obo REE deposit was discovered in 1927 as a Fe deposit (3). Currently both Fe and REEs are mined; Nb ore is also present. The deposit is located in Inner Mongolia, at  $41^{\circ}45'N$  and  $110^{\circ}E$ . The mine is owned and operated by the Baotou Iron and Steel Corporation of the Ministry of Metallurgical Industry of the People's Republic of China.

The rocks of the Middle Proterozoic Bayan Obo Group, which hosts the ore, represent a platform sequence on the northern flank of the Archean Sino-Korean craton. Sedimentary rocks of the sequence were probably deposited in an E-W-trending graben or trench, with the open sea to the north (4), and then uplifted and regionally metamorphosed at about 1.4 Ga (5).

Geologically, the Bayan Obo region (Fig. 1) can be divided into two parts: (a) north of the Kuangou fault zone is an unmineralized, weakly regionally metamorphosed limestone and shale sequence H1-H10 (Hu in Fig. 1) (6); and (b) south of the Kuangou fault zone the mine region is more strongly regionally metamorphosed and includes the Bayan Obo

Group, which is 1,880 m thick and consists of a sequence of quartzite, slate and shale, and crystalline dolomite (H1-H9, Fig. 1). The H9 black slate and shale south of the fault zone is in the trough of a syncline, and is underlain and flanked on both sides by the highly mineralized H8 dolomite. The striking differences in lithology, structural pattern, and mineralization north and south of the fault zone indicate a post-ore-formation age for the Kuangou fault.

Both REE ores and Fe-REE ores are stratabound within the H8 dolomite (Fig. 1). The dolomite ranges from 240 to 540 m in thickness, and is overlain by the relatively impervious, 340-360 m thick, H9 black slate and shale (Fig. 1), which may have acted as a caprock for the mineralizing solutions. The dolomite strikes E-W for about 16 km and is approximately 1-2 km in width in the N-S direction. The Main Ore Body and East Ore Body (Fig. 1) are located where the H8 dolomite is thickest.

In the field, the ores were not found to be associated with any plutonic or volcanic rocks, and there has been no observed occurrence of alkalic granitic or subsilicic alkalic rocks in and adjacent to the mine region. Field and laboratory evidence indicates that the ore-bearing rocks have suffered both pre- and post-ore regional metamorphism.

Mineral paragenetic sequence and ages of mineralization. Four independent methods were used to determine the mineral paragenetic sequence and ages of mineralization of the deposit: (a) field observations, (b) detailed petrographic textural analysis, (c) radio-isotopic determination of mineral ages, and (d) chemical analysis of minerals determined by the preceding three methods to be of different generations in the mineral paragenetic sequence.

Field and laboratory evidence indicates that the H8 host dolomite is of sedimentary origin (4, 7, 8), and not a carbonatite as previously suggested (3, 9, 10). This evidence includes: (a) conformable contacts of the dolomite with the overlying H9 black slate and shale and the underlying H7 mica schist and dolomite; (b) general massive appearance of the H8 dolomite, with occasional interbeds and lenses of quartzite, scattered detrital quartz, and rounded detrital apatite grains in planes parallel to the bedding; (c) presence, although rare, of algae microfossils in the dolomite (7); and (d) nature of the dolomite: ferroan (FeO 3-7 wt %), dominantly very fine-grained and well recrystallized (11). The  $^{18}\text{O}$  values for the H8 dolomite range from +12 to +16 ‰ (SMOW), and presumably were induced by interaction with hydrothermal solutions of light O isotopic composition.

The mineralogy of the Bayan Obo ores is extremely complex, as shown by the fact that more than 100 minerals have been described from this deposit (12). The most important REE ore minerals of Bayan Obo are monazite ((Ce,La,Nd)PO<sub>4</sub>), bastnaesite ((La,Ce)(CO<sub>3</sub>)F), and huanghoite (BaCe(CO<sub>3</sub>)<sub>2</sub>F); the most important Fe minerals are magnetite (Fe<sub>3</sub>O<sub>4</sub>) and hematite (Fe<sub>2</sub>O<sub>3</sub>); and the most important Nb ore minerals appear to be fergusonite (YNbO<sub>4</sub>), aeschynite ((Ce,Ca,Fe,Th)Nb<sub>2</sub>(O,OH)<sub>6</sub>), and columbite (FeNb<sub>2</sub>O<sub>6</sub>) (see (12)).

The two major types of dolomite-hosted REE and REE-Fe ores are: (a) disseminated REE ore, and (b) finely laminated and banded high-grade REE and REE-Fe ore that occurs in pods and lenses (Fig. 2). In addition, massive Fe ores with very low REE content occur in the central part of the major ore bodies and in the western part of the mine region. Mineral zoning is not apparent in the ore bodies (13). RE<sub>2</sub>O<sub>3</sub> contents

in the disseminated ores range from 2 to 6 wt %. In the banded ores and some massive Fe ores, ore grades vary from 2 to 25 wt % RE<sub>2</sub>O<sub>3</sub> and from 20 to 55 wt % Fe (averaging about 34 wt % Fe) (13).

Replacement textures are widespread and are observable both megascopically and microscopically. The earliest introduction of stringers and sheaths of very fine-grained monazite aggregates, which preceded the introduction of magnetite in the mineral paragenetic sequence, came after recrystallization of the dolomite into a marble. For example, in the field, yellow streaks and irregular lacy networks of very fine-grained monazite were seen in essentially pure dolomite. Irregular patches of magnetite within dolomite and irregular boundaries between magnetite-rich areas and the dolomite host were also widely observed. Microscopically, fine-grained granular monazite occurs interstitially along dolomite triple-junction grain boundaries, destroying the host fabric by replacing the dolomite crystals (Figs. 3A and 3B). Where magnetite occurs in H8 dolomite that contains early monazite, the magnetite is interstitial between grains of dolomite and monazite (Fig. 4A). Where strongly twinned dolomite crystals occur with magnetite, the irregularly shaped relict dolomite remains in continuous optical orientation surrounded by the replacing magnetite (Fig. 4B). Similar destruction of the triple-junction grain boundary fabric of the host dolomitic marble by other minerals, such as magnesio-arfvedsonite, aegirine, phlogopite, fluorite, barite, apatite, and hematite, is also widespread. Banded ores are cut by veins of younger aegirine, with or without magnesio-arfvedsonite, and contain large huanghoite and aeschynite crystals. No evidence indicating a syngenetic origin for the ores, such as oolitic textures in Fe ores, was found.

On the basis of field and microscopic textural analysis of disseminated and banded ores and radioisotopic dating of minerals, the generalized principal mineral paragenetic sequence (8) was determined to be: (a) magnesio-arfvedsonite,  $802 \pm 19$  Ma (1, Table 1); (b and c) disseminated monazite, earlier than magnesio-arfvedsonite with an age of  $628 \pm 15$  Ma (2, Table 1); (d) disseminated monazite,  $594 \pm 4$  Ma (5, Table 1); (e) magnesio-arfvedsonite,  $440 \pm 11$  Ma (3, Table 1); (f) early magnetite; (g) granular hematite; (h) magnesio-arfvedsonite, monazite, and bastnaesite,  $425 \pm 10$  Ma (4, 6, and 7, Table 1); (i) late magnetite; (j) vein huanghoite and aeschynite,  $438 \pm 25$  Ma (see below); and (k) Hercynian late-stage mineral assemblages including sulfides, microcline, albite, phlogopite, fluorite, barite, quartz, calcite, fergusonite, rare Ba and Sr REE fluorocarbonates, and Ba and Sr carbonates. Episodes of REE mineralization appear to be separate in time from those of Fe mineralization. Niobium mineralization occurred during and after the second stage of magnetite mineralization (stages i, j, and k).

In general, radioisotopic ages (Table 1) are consistent with the texturally determined mineral paragenetic sequence. Mineral ages listed in Table 1 are considered to be minimum ages because later heating events may have resulted in a slight reduction of the radioisotopic ages.

It is important to note that the K/Ar and <sup>40</sup>Ar/<sup>39</sup>Ar ages of the four magnesio-arfvedsonites (Table 1) cover a span of about 400 million years and that these samples have distinctly different chemical characteristics, varying from MgO>FeO to MgO<FeO, coupled with MnO<sub>2</sub> content ranging from 0.06 to 5.68 wt %. Such distinct compositions suggest that each generation of amphibole was deposited by a different

Table 1. Chemical compositions\* and ages of selected Bayan Obo minerals (ages in Ma).

Sample No.	Magnesio-arfvedsonites				Monazites		Bastnaesite	
	(1) 40-14	(2) 796-48-277	(3) 8B42-10	(4) 7B34-1	(5) 12-6	(6) 7B31-9	(7) 7B30-3	
SiO <sub>2</sub>	56.55	53.85	55.96	57.09	F	0.85	1.05	12.69
TiO <sub>2</sub>	0.04	0.04	--	--	La <sub>2</sub> O <sub>3</sub>	17.07	22.89	24.28
Al <sub>2</sub> O <sub>3</sub>	0.59	0.44	0.48	0.34	BaO	--	--	0.10
FeO	13.24	12.59	15.48	12.80	Nd <sub>2</sub> O <sub>3</sub>	12.85	9.54	9.16
MnO	0.13	5.68	2.82	0.06	Ce <sub>2</sub> O <sub>3</sub>	35.84	34.63	37.75
MgO	15.96	12.47	12.88	16.63	Pr <sub>2</sub> O <sub>3</sub>	3.98	2.90	3.29
CaO	0.61	1.92	1.77	0.23	Y <sub>2</sub> O <sub>3</sub>	0.08	0.20	0.08
Na <sub>2</sub> O	7.03	7.64	7.19	8.11	P <sub>2</sub> O <sub>5</sub>	29.77	29.24	--
K <sub>2</sub> O	<u>2.93</u>	<u>1.90</u>	<u>2.21</u>	<u>1.16</u>	-O=F	<u>0.36</u>	<u>0.44</u>	<u>5.34</u>
Total	97.08	96.53	98.81	96.45		100.19	100.07	82.07

K/Ar ages	802±19	628±15	440±11		Analysts: Tianjin lab.	
<sup>40</sup> Ar/ <sup>39</sup> Ar ages			425±10		Analysts: McKee & Turrin	
Th/Pb ages	Analysts: Tatsumoto & Li			594±4	426±6	426±6

\*All analyses are averages, expressed in wt %, by electron probe microanalysis; total iron is expressed as FeO; analysts: J.M. Back and J.A. Minkin.

--Below limit of detection (MDL); MDL for TiO<sub>2</sub> = 0.04, BaO = 0.05, P<sub>2</sub>O<sub>5</sub> = 0.04, all in wt %.

hydrothermal solution. Although post-mineral-formation heating of magnesio-arfvedsonites may have slightly reset the isotopic ages, this could not account for the distinctions in chemical compositions.

The dated magnesio-arfvedsonites have been used to refine the texturally derived mineral paragenetic sequence. For example, magnesio-arfvedsonite of age 628 ± 15 Ma (2, Table 1, and Fig. 5) is younger than monazite inclusions in the amphibole and older than magnetite that truncates it.

Most of the REE minerals of Bayan Obo contain less than 25 ppm U, and thus they are not datable by U/Pb methods. However all of the monazites and bastnaesites analyzed for ThO<sub>2</sub> (13) contained between 0.1 and 0.7 wt % ThO<sub>2</sub>, sufficient for Th/Pb dating. Compositions of the Bayan Obo monazites and bastnaesites are dominated by light REEs and typically have very steep REE distribution patterns when normalized to chondrites (3). The two monazites in Table 1 have distinctly different Th/Pb ages as well as different La<sub>2</sub>O<sub>3</sub> (17.1 vs. 22.9 wt %) and Nd<sub>2</sub>O<sub>3</sub> (12.8 vs. 9.5 wt %) concentrations. Again, radioisotopic ratios may have been affected (but to a lesser extent than the amphiboles (14,15)) by heating subsequent to crystallization, without significantly modifying the REE compositions of the monazite.

An age of  $426 \pm 6$  Ma was determined from a four-point Th/Pb mineral isochron for two monazites (one pure and one impure sample) from a banded ore (6, Table 1) and bastnaesite (7, Table 1) and apatite from another banded ore sample from a nearby locality. Two samples each of huanghoite and aeschynite from aegirine veins cross-cutting banded ore (stage j in the paragenetic sequence) were dated by the Th/Pb and Sm/Nd methods. A four-point Th/Pb isochron for these samples gave an age of  $438 \pm 25$  Ma. The Sm/Nd age for the same minerals ( $418 \pm 96$  Ma) is in general agreement with the Th/Pb results. Because of the large uncertainties for these determinations, the isotopic age of the cross-cutting veins cannot be distinguished from that of the monazite-bastnaesite-apatite of the banded ore.

Comparison of Bayan Obo mineral characteristics with those of known magmatic origin. Crystalline REE deposits are commonly associated with alkaline and carbonatite igneous rocks (16). Therefore, one might assume that the REE and Fe of the Bayan Obo deposit were derived from hydrothermal solutions related to a carbonatite or alkalic magma at depth. However, no alkalic igneous rocks have been found in or near the mine region. In addition, apparent dissimilarities exist between Bayan Obo mineral compositions and those from other localities associated with alkalic granites and carbonatites. For example,  $\text{ThO}_2$  is generally less than 0.7 wt % in Bayan Obo monazites and bastnaesites, but on the average 2.1 wt %  $\text{ThO}_2$  is present in monazites in carbonatites (Table 2), and 4.8 wt % in monazites in alkalic granites (17). Additional differences in chemical characteristics of Bayan Obo minerals vs. those from carbonatites are listed in Table 2.

Conclusions. (a) The H8 host crystalline dolomite was not a magmatic carbonatite, but rather was probably deposited as a carbonate sediment in Middle Proterozoic time. The carbonate was later dolomitized. The mine region was subsequently regionally metamorphosed, converting the dolomite to a well recrystallized marble prior to mineralization. (b) The Bayan Obo ore deposit is hydrothermal, metasomatic, and epigenetic in origin. (c) Episodes of hydrothermal REE, Fe, and Nb mineralization occurred repeatedly during a time span of about 400 million years. The peak of mineralization of REE and Fe was between about 440 and 425 Ma (Caledonian time).

Additional data and further comparison of chemical compositions, initial isotopic ratios of REE minerals, and mineral paragenetic sequence of Bayan Obo with REE deposits of known magmatic or hydrothermal origin may help to determine the source of the REEs in the Bayan Obo deposit. At present the data for the Bayan Obo deposit suggest that it is unique in its geologic setting, origin, complex mineral paragenetic sequence, and multiple episodes of mineralization that occurred over a span of hundreds of millions of years.

Table 2. General comparison of mineral characteristics between Bayan Obo and carbonatites.

Bayan Obo	Carbonatites
1. Monazites contain typically very low ThO <sub>2</sub> (<0.7 wt %).	1. Monazites contain an average of 2.1 wt % ThO <sub>2</sub> (13).
2. Magnetites typically contain very low TiO <sub>2</sub> (<0.1 wt %)	2. Magnetites contain a wide range of TiO <sub>2</sub> (e.g. 0.51-16.8 wt %, Magnet Cove, AR (18, 19), and 0.9 wt %, African carbonatites (20)).
3. Alkali amphiboles are alumina-poor magnesio-arfvedsonites.	3. Wide range of amphiboles: from alumina-rich hastingsites to alumina-poor arfvedsonites (21).
4. Principal minable REE-minerals are monazite, bastnaesite, and huanghoite.	4. Except bastnaesite of Mountain Pass, CA, REE's are mostly concentrated in apatites and pyrochlore (21).
5. Principal potentially minable niobium minerals are fergusonite, aeschynite, and columbite.	5. Principal niobium mineral is pyrochlore (21).

## REFERENCES AND NOTES

1. Mike O'Driscoll, Industrial Minerals, pp. 21-55 (1988).
2. E. Chin, in Minerals Yearbook, v. III, Area Reports: International (U.S. Bureau of Mines, 1985), pp. 209-236.
3. Bai Ge and Yuan Zhongxin, Bulletin of the Institute of Mineral Deposits, no. 13 (Chinese Academy of Geological Sciences, 1985), pp. 107-140 in Chinese, English abstract pp. 189-192.
4. Meng Qingrun, Geological Review, v. 28, no. 5, pp. 481-489 (1982), in Chinese with English abstract.
5. Wang Hongzhen et al., Atlas of the paleogeography of China (Cartographic Publishing House, Beijing, China, 1985), pp. 1-85 in Chinese, pp. 1-24 in English. Legend to maps in Chinese and English.
6. In accordance with Chinese convention, Middle Proterozoic is designated as "H" in this paper; this notation is retained in the text for easy reference with respect to existing Chinese literature. U.S. Geological Survey notation however, designates Proterozoic as "Y."
7. Hou Zonglin, Research on ore genesis of the Bayan Obo ore deposit of Inner Mongolia, China (Tianjin Geological Research Academy, Ministry of Metallurgical Industry, 1987), 10 pp. in Chinese.
8. E.C.T. Chao et al., in U.S. Geol. Survey Circular 1035, K.S. Schindler, Ed. (U.S. Geological Survey, Denver, 1988), pp. 8-10.
9. Zhou Zhenlin, Li Gongyuan, Sung Tongyun, and Liu Yuguang, Geological Review, v. 26, no. 1, pp. 35-41 (1980), in Chinese.
10. Liu Tie Gen, Geological Review, v. 32, no. 2, pp. 150-159 (1986), in Chinese with English abstract.
11. E.C.T. Chao et al., Abstracts, Geol. Soc. of America, 1988 Annual Meeting, Denver (Geol. Soc. of America, Boulder, CO, 1988), p. A143.
12. Zhang Peishan and Tao Kejie, Bayan Obo Mineralogy (Science Press, Beijing, 1986), pp. 1-182 in Chinese, English summary pp. 199-208.
13. E.C.T. Chao et al., Abstracts of the 28th Int. Geol. Congress, 9 to 19 July, 1989 (International Geological Congress, Washington, D.C., 1989), v. 1, p. 262.
14. G.K. Muecke, C. Pride, and P. Sarkar, in Rare Earth Element Geochemistry of Regionally Metamorphic Rocks, L.H. Ahrens, Ed. (Pergamon Press, Oxford, 1979), pp. 449-464.
15. C.J. Hawkesworth and P.W.C. Van Calsteren, in Rare Earth Element Geochemistry, P. Henderson, Ed. (Elsevier, 1984), pp. 375-421.
16. C.R. Neary and D.E. Highley, in Rare Earth Element Geochemistry, P. Henderson, Ed. (Elsevier, 1984), pp. 423-466.
17. M. Fleischer and S. Rosenblum, written communication, 1989.
18. R.L. Erickson and L.V. Blade, U.S. Geol. Survey Prof. Paper 425 (U.S. Gov't. Printing Office, Washington, D.C., 1963).
19. M.J.K. Flohr and Malcolm Ross, submitted to Lithos.
20. P. Prins, Lithos, 5, pp. 227-240 (1972).
21. Keith Bell, ed., Carbonatites Genesis and Evolution (Unwin Hyman Ltd., London, 1989).
22. Geologic map modified from L.J. Drew and Q. Meng, U.S. Geol. Survey Misc. Inv. Series I-2057, in press; Q. Meng, written communication, 1989.

23. Acknowledgment: We thank Zhang Guozhong, president and manager of the Baotou Iron and Steel Company for permission to conduct field work at Bayan Obo in the summers of 1987 and 1988. We thank Liu Liu, chief engineer of Baogang, and mine geologists Huang Shengguang and Wu Janjiang for assisting us in collecting more than 800 samples used in this study. We thank our colleagues L.J. Drew and Meng Qingrun for the use of the Bayan Obo regional geologic map cited in item 22, and Paul Barton and W.C. Shanks for valuable suggestions made in reviewing this paper.

This study was undertaken as a joint project under the Earth Sciences Protocol, between the Geologic Division of the U.S. Geological Survey of the United States and the Tianjin Geological Research Academy of the Ministry of Metallurgical Industry of the People's Republic of China.

## ILLUSTRATIONS

Figure 1. Geologic map of the Bayan Obo area (22).

Figure 2. Photograph of a block of typically laminated and banded ore from the East Ore Body, with iron oxide (fe), fluorite (f), and REE minerals plus aegirine (r).

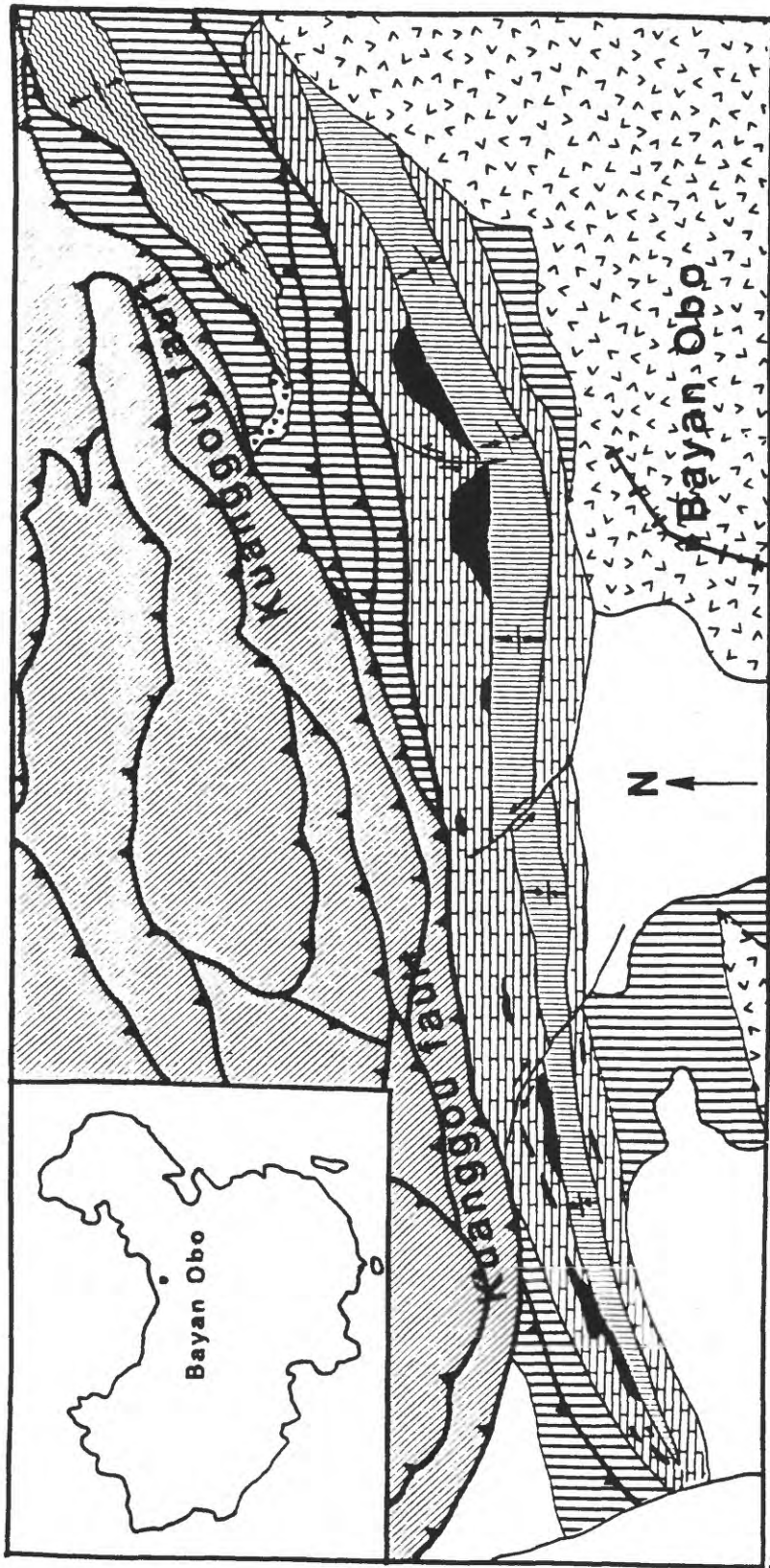
Figure 3A. Photomicrograph of very fine-grained H8 dolomite with dark sub-parallel to branching streaks consisting of extremely fine-grained monazite. Transmitted light (TL).

Figure 3B. Photomicrograph of an enlargement of a portion of Fig. 3A showing the elongation of the dolomite grains (d), and the interstitial and streaky occurrence of monazite (m) along the sub-parallel microfractures in the dolomite. TL, X-nicols (XN).

Figure 4A. Photomicrograph of H8 dolomite illustrating sequence of replacement: monazite (m) partially replacing dolomite (d), and magnetite (mt) interstitially replacing dolomite (d) and monazite (m). Reflected light (RL).

Figure 4B. Photomicrograph showing magnetite (mt) partially replacing an optically continuous twinned dolomite crystal. TL, XN.

Figure 5. Photomicrograph of alkali amphibole (a) with a K/Ar age of  $628 \pm 15$  Ma (sample 796-48-277, Table 2). Notice the small round monazite inclusions (m) in the amphibole, and truncation and replacement of the amphibole by late-stage magnetite (mt).



MAP EXPLANATION

- |              |   |
|--------------|---|
| ore bodies   | Tertiary sedimentary rocks  |
| syncline     | Permian (Hercynian) diorite                                       |
| anticline    | Permian (Hercynian) granitic rocks                                |
| thrust fault | Y9 (H9) slate-shale south of Kuanggou fault                       |
| fault        | Y8 (H8) dolomite south of Kuanggou fault                          |
|              | Y1-Y7 (H1-H7) undifferentiated sequence south of Kuanggou fault   |
|              | Archean gneisses (Wutai Group) south of Kuanggou fault            |
|              | Y1-Y10 (H1-H10) undifferentiated sequence north of Kuanggou fault |

